Bremsstrahlung induced by proton and ^{3}He-ion bombardments in the 1–4-MeV/amu energy range

K. Ishii and S. Morita
Department of Physics, Tohoku University, Sendai, Japan

H. Tawara
Department of Nuclear Engineering, Kyushu University, Fukuoka, Japan

(Received 17 April 1975; revised manuscript received 29 July 1975)

Continuous x rays from a thin aluminum target produced by proton and ^{3}He-ion bombardments have been measured with a Si(Li) detector over the impact-energy ranges 1–4 MeV and 3–9 MeV, respectively. The experimental results obtained were compared with theoretical predictions based on the binary-encounter approximation. Agreements are obtained both in the shape of spectra and absolute cross sections without any adjustable parameter over the entire energy range measured, but generally the theoretical calculation predicts smaller cross sections than the experimental results as the photon energy becomes higher and the bombarding energy gets lower. Energy-dependent directional anisotropy of the bremsstrahlung was theoretically estimated and compared with the experimental results measured at directions 45°, 90°, and 135° with respect to the incident beam, showing qualitative agreement.

I. INTRODUCTION

Recently it has been found that the continuous x rays induced by heavy–charged-particle bombardment of solid targets play an important role as the background for the detection of characteristic x rays in element analyses, resulting in a severe limit on the concentration which can be measured,[1,2] and also for the identification of the quasimolecular orbital (MO) x rays produced in heavy-ion–atom collisions, since the continuous MO x rays overlap the high-energy tail of the continuous bremsstrahlung.[3–5]

These continuous radiations are mainly composed of (i) bremsstrahlung from secondary electrons ejected by the projectile, (ii) bremsstrahlung which occurs during close collisions between the projectile and the target nucleus, and (iii) low-energy photons from the Compton scattering of γ rays from nuclear excited states. The first type of radiation is generally most predominant. The second type becomes of interest at higher radiation energies. The third type is strongly dependent on the target nucleus and experimental arrangement, and can sometimes be of similar importance as the second type or become predominant as the projectile energy gets higher. Intensity of the first type of radiation is very strong at low radiation energies, but decreases rapidly when the photon energy becomes larger than $T_m = 4m_e E_p/M_p$, which represents the maximum energy that can be transferred from a projectile of mass M_p and energy E_p to a free electron of mass m_e. The continuous radiation in the region above T_m is produced by the energetic secondary electrons ejected from target atoms. These electrons come from the strongly bound orbits, where before the impact they already have high velocities.

From the point of view of element analysis, Folkmann *et al.*[1] have measured the continuous x rays in the region above 2 keV with proton bombardments at 2 and 3 MeV on carbon and aluminum targets and compared the results with their theoretical calculations.

Our aim here is to measure the continuous radiation with proton and ^{3}He-ion bombardments on an aluminum target over the energy ranges 1.0–4.0 MeV and 3–9 MeV, respectively, and to compare the results with the calculation of improved approximations. Not only the shape of spectra, in which Folkmann *et al.* are mainly interested, but also the absolute cross sections for bremsstrahlung production are compared with the experimental results. The angular dependence of the spectrum will also be estimated and compared with the experimental results.

II. EXPERIMENT AND RESULTS

A self-supporting 110-μg/cm^2 Al target was bombarded with proton and ^{3}He-ion beams from the 5-MV Van de Graaff accelerator of Tohoku University. The thickness of the target was measured by the Rutherford scattering of 1.0-MeV protons and by weighing with a microbalance. An Ortec Si(Li) detector had a resolution of 205 eV at 6 keV, an effective area of 12.5 mm^2, and a 0.001-in.-thick Be window. The x rays passed through a Mylar vacuum-chamber window of 10 μm and air paths of 26.2 and 26.0 mm for proton and ^{3}He-ion experiments, respectively, before

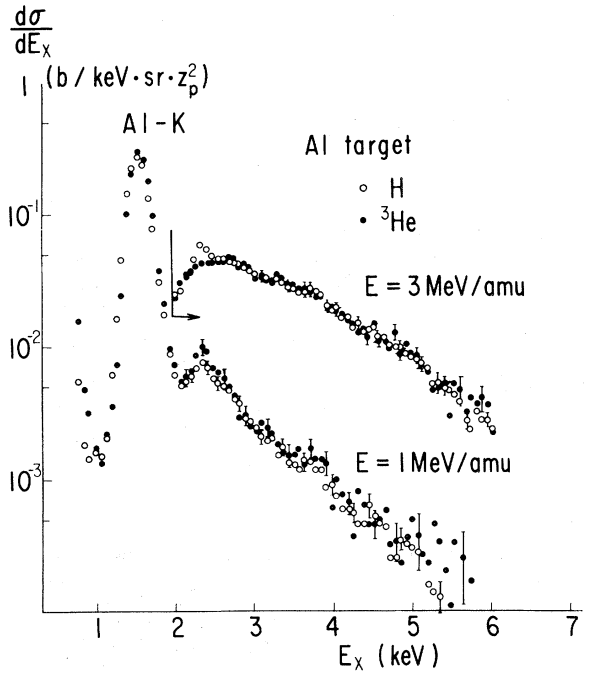

FIG. 1. X-ray spectra, measured at the direction of 90°, from an Al target bombarded by proton and ^{3}He beams. Corrections for absorption of x rays in the Mylar window and the air path and for the detection efficiency have not been made. The x-ray intensity is scaled by the nuclear charge Z_p of the incident particle.

entering the detector. In order to monitor possible target deterioration during the bombardment, elastically scattered particles were simultaneously measured with a solid-state detector. The counting rate had been kept below 100 cps to avoid piling-up effect.

Typical spectra obtained at bombarding energies of 1 and 3 MeV/amu and at an angle of 90° with respect ot the incident beam are presented in Fig. 1, where the background, which was measured without the target, has been subtracted but the corrections for absorption of x rays and for the detector efficiency have not been done. The ordinate

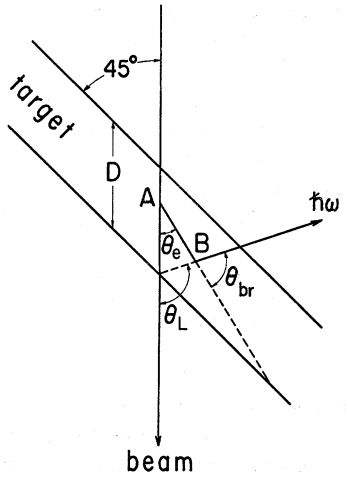

FIG. 2. An incident particle ejects an electron of energy E_e at point A to the direction θ_e with respect to the incident beam, and the electron loses its energy down to E'_e at point B, where it produces bremsstrahlung of energy $\hbar\omega$ to the direction θ_{br} with respect to the direction of the electron and to the direction θ_L with respect to the incident beam. The thickness of the target is $D/\sqrt{2}$.

of Fig. 1 shows b/keV sr Z_p^2, where Z_p is the projectile charge. As seen in this figure, the continuous x-ray spectrum can be well scaled by the projectile velocity E/amu and the intensity is proportional to Z_p^2. The small peak appearing at 2.3 keV might be due to S $K\alpha$ (2.307 keV) x rays from sulfur impurity in the target.

III. THEORETICAL

A. Bremsstrahlung from secondary electrons

Secondary electrons are produced in the target by collisions of a projectile with free electrons or by ionization of bound electrons in the target atom. Referring to Fig. 2, the production cross section of bremsstrahlung σ^{SEB} by secondary electrons is expressed by

$$\frac{d\sigma^{SEB}}{d(\hbar\omega)\,d\Omega_L} = \int dE_e \int d\Omega_e \int dE'_e \left[\frac{d\sigma^{br}}{d(\hbar\omega)\,d\Omega_{br}}(E'_e, \hbar\omega, \theta_{br})\left(\frac{-N\,dx}{dE'_e}\right)\frac{d\sigma_e(E_e, \theta_e)}{dE_e\,d\Omega_e}\right]. \quad (1)$$

Here Ω_L is the laboratory solid angle subtended by the detector, σ^{br} is the bremsstrahlung-production cross section for an electron of energy E'_e, and $\sigma_e(E_e, \theta_e)$ is the electron-ejection cross section for the projectile. The indices br and e refer to bremsstrahlung and electron, respectively, and $-dE'_e/N\,dx$ is the energy loss of the electron divided by the number of target atoms per unit volume N, and is given by Bethe as[6,7]

$$-\frac{dE'_e}{N\,dx} = \frac{4\pi e^4}{m_e v^2} Z \ln\left(\frac{1.16}{\bar{I}} E'_e\right), \quad (2)$$

where m_e, e and v are the mass, charge, and velocity of a secondary electron, respectively,

and Z and $\bar{I}$ are the atomic number and the mean excitation energy of the target atom, respectively; here, we took $\bar{I}=163$ eV.[7]

The bremsstrahlung-production cross section given by Heitler[8] is applicable for the case of $Ze^2/\hbar v \ll 1$, whereas in the present case $Ze^2/\hbar v \approx 1$. The semiclassical calculation by Jackson[9] gives the cross section for our case, at the high-energy limit $E'_e = \hbar\omega$, as

$$\frac{d\sigma^{\mathrm{br}}}{d(\hbar\omega)\,d\Omega_L} = \frac{2}{\pi}\frac{Z^2e^2}{\hbar c}\left(\frac{e^2}{m_e c^2}\right)\left(\frac{c}{v}\right)^2\frac{1}{\hbar\omega}\ln\left(4\frac{E'_e}{\hbar\omega}\right)\sin^2\theta_{\mathrm{br}}. \tag{3}$$

In the integrand of Eq. (1), the main contribution to the integral comes from the region where the photon energy $\hbar\omega$ is comparable to the electron energy E'_e. Thus Eq. (3) can approximately be assumed for the bremsstrahlung production. In order to examine the validity of this approximation, values of the maximum differential and total cross sections for a case $E'_e = 5$ keV and $\hbar\omega = 4$ keV in Al target, given by Eq. (3), were compared with those given by the formula of Tseng and Pratt,[10] which is derived from the HFS calculation and has been proven to give excellent agreement with experimental results obtained in the region $E'_e > 10$ keV: It was found that both results are in agreement within an accuracy of about 10%. It must be noted, however, that the angle corresponding to the maximum differential cross section given by Tseng and Pratt is about 75°, in contrast to 90° given by Eq. (3), because of the retardation effect, which has been neglected in Eq. (3).

The ejection cross section of an electron of energy E_e from a target atom by the projectile, $d\sigma_e(E_e, \theta_e)/dE_e\,d\Omega_e$, can be estimated from the BEA[11] or PWBA[12] theories, and the cross section calculated from the BEA by Bonsen and Vriens[13] was used here.

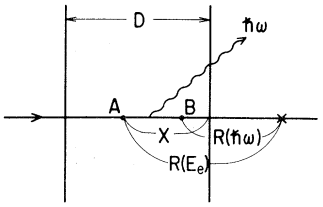

FIG. 3. At point A, which is a distance x from the target surface, the projectile ejects an electron of energy E_e to the forward direction, where the differential cross section for electron ejection has a pronounced maximum, and loses its energy down to $\hbar\omega$ at point B. R is the range of the electron in the target as a function of energy. In the case where point B is outside of the target, i.e., $x \geq R(E_e) - R(\hbar\omega)$, the effect of escape of electrons from the target is to be taken into account.

Referring to Fig. 3, which shows the case of electron ejection to the forward direction, where the differential cross section is maximum, the integration limits for E_e and E'_e in Eq. (1) were taken as follows: (a) For the case of $x \geq R(E_e) - R(\hbar\omega)$, i.e., $\hbar\omega \leq E_e \leq E_e^{\max}$,

$$\int_{\hbar\omega}^{E_e^{\max}} dE_e \int_{\hbar\omega}^{E_e} dE'_e \ldots,$$

where $R(E_e) \cong 2.138E_e^2$ μg/cm^2 (E_e in keV)[14] is the range of electrons of energy E_e in aluminum, and $R(E_e^{\max}) = R(\hbar\omega) + x$ and $E_e^{\max} = [(x/2.138) + (\hbar\omega)^2]^{1/2}$ (x in μg/cm^2); (b) For the case of $x \leq R(E_e) - R(\hbar\omega)$, i.e., $E_e^{\max} \leq E_e < \infty$,

$$\int_{E_e^{\max}}^{\infty} dE_e \int_{E_e^{\min}}^{E_e} dE'_e \ldots,$$

where $R(E_e^{\min}) = R(E_e) - x$, and $E_e^{\min} = (E_e^2 - x/2.138)^{1/2}$.

Therefore, by taking into account the effect of escape of electrons from the target, we obtain

$$\frac{1}{D}\int_0^D dx\left(\int_{E_e^{\max}(x)}^{\infty} dE_e \int_{E_e^{\min}(x)}^{E_e} dE'_e \ldots + \int_{\hbar\omega}^{E_e^{\max}(x)} dE_e \int_{\hbar\omega}^{E_e} dE'_e \ldots\right)$$
$$= \int_{\hbar\omega}^{\infty} dE_e \int_{\hbar\omega}^{E_e} dE'_e \ldots - \frac{1}{D}\int_0^D dx \int_{E_e^{\max}(x)}^{\infty} dE_e \int_{\hbar\omega}^{E_e^{\min}(x)} dE'_e \ldots. \tag{4}$$

The second term of the above equation shows the effect of escape of electrons from the target; it amounts to only several percent in the region $\hbar\omega < 10$ keV. But in the region of several tens of keV, where the contribution from MO x rays becomes important, the second term becomes comparable to the first. By using the relation $\sin^2\theta_{\mathrm{br}} = 1 - (\cos\theta_e \cos\theta_L + \sin\theta_e \sin\theta_L \cos\varphi_e)^2$ (see Fig. 2) and the isotropy[13] of $d\sigma_e/dE_e d\Omega_e$ with respect to φ_e, φ_e being the azimuthal angle for θ_e, Eq. (1) leads to

$$\frac{d\sigma^{\mathrm{SEB}}}{d(\hbar\omega)\,d\Omega_L} \simeq (3C_2 - C_1)\sin^2\theta_L + 2(C_1 - C_2), \tag{5}$$

with

$$C_1 = \frac{3}{8}\int_{\hbar\omega}^{\infty} dE_e \int_{\hbar\omega}^{E_e} dE'_e \int_0^{\pi} d\theta_e \left[\frac{d\sigma^{br}}{d(\hbar\omega)}\left(\frac{-N\,dx}{dE'_e}\right) \times \frac{d\sigma_e}{dE_e\,d\Omega_e}\sin\theta_e\right],$$

and

$$C_2 = \frac{3}{8}\int_{\hbar\omega}^{\infty} dE_e \int_{\hbar\omega}^{E_e} dE'_e \int_0^{\pi} d\theta_e \left[\frac{d\sigma^{br}}{d(\hbar\omega)}\left(\frac{-N\,dx}{dE'_e}\right) \times \frac{d\sigma_e}{dE_e\,d\Omega_e}\cos^2\theta_e \sin\theta_e\right].$$

Thus the angular distribution of ejected electrons was taken into account.

In estimating the cross section given by Bonsen and Vriens,[13] the velocity distribution of the bound electrons was taken from the hydrogenic wave function of velocity representation. The results of the calculations for an Al atom at bombarding energies of $E/\text{amu} = 1.0$ and 4.0 MeV are presented in Figs. 4 and 5, respectively; the results are

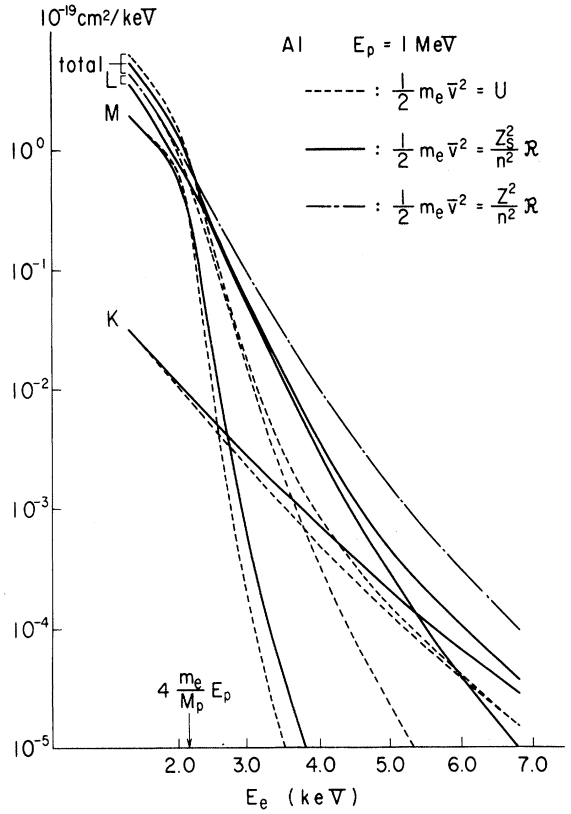

FIG. 4. Energy distribution of electrons ejected from an Al atom by 1-MeV proton bombardment calculated from the BEA theory. Calculations were carried out for three values of the mean velocity of the bound electrons, shown in the figure, and the partial cross sections for each shell are shown for two of the three.

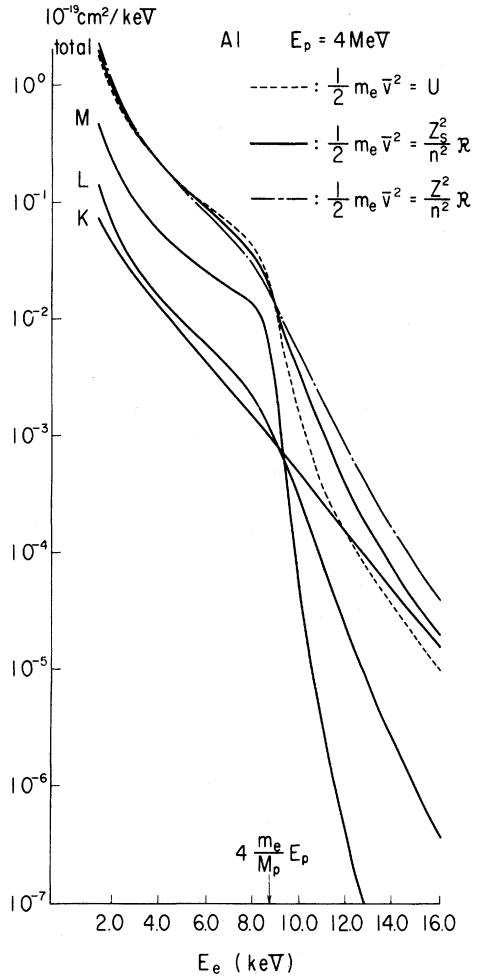

FIG. 5. Same as in Fig. 4, except $E_p = 4$ MeV.

shown for three values of the mean velocity of bound electrons, v, given by

$$\tfrac{1}{2}m_e\bar{v}^2 = U, \tag{6a}$$

$$\tfrac{1}{2}m_e\bar{v}^2 = (Z_s^2/n^2)\mathcal{R}, \tag{6b}$$

$$\tfrac{1}{2}m_e\bar{v}^2 = (Z^2/n^2)\mathcal{R}. \tag{6c}$$

Here U is the measured binding energy of the electrons, Z_s is the effective nuclear charge calculated from Slater's screening rules, Z is the nuclear charge, n is the principal quantum number for each subshell, and $\mathcal{R}$ is the Rydberg energy.

It is seen in Figs. 4 and 5 that the electrons ejected from outer shells are predominant in the energy region below $T_m = 4m_eE_p/M_p$, whereas the electrons from the inner shells are predominant in the region above T_m and rather large differences in the electron-ejection cross section are seen for the three values of $\bar{v}$ in contrast to the region be-

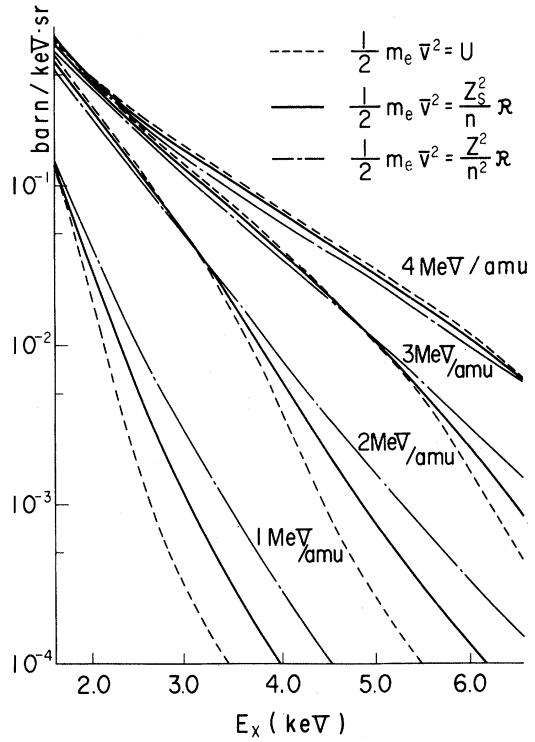

FIG. 6. Bremsstrahlung spectra produced by the secondary electrons calculated from the BEA theory for the three values of the mean velocity of the bound electrons. The parameter shows the bombarding energy.

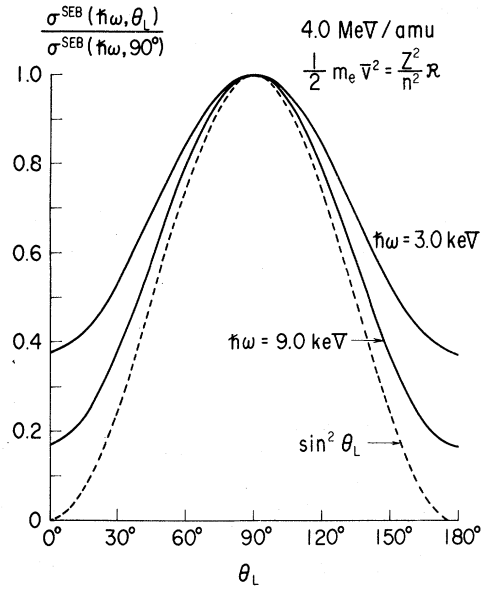

FIG. 7. Calculated angular dependence of the bremsstrahlung produced by the secondary electrons for the bombarding energy 4.0 MeV/amu. The ratios of the cross section for the bremsstrahlung production at an angle θ_L to that at 90^0 were plotted for photon energies of 3.0 and 9.0 keV and infinity.

low T_m. Thus the electrons ejected from the K shell are most predominant in the region above 10 keV for $E_p = 4$ MeV and in the region above 5 keV for $E_p = 1$ MeV. According to the experimental results on the electrons ejected from neon atoms at $E_p = 50$, 100, and 300 keV by Rudd *et al.*,[15] the mean velocity defined by Eq. (6b) gives better agreement in the region $E_e > T_m$ than that defined by Eq. (6a). Moreover, as the electrons in an aluminum atom are bound closely to the nucleus, the screening effect for the nuclear charge would be neglected in the region where the electrons ejected from the inner shell mainly contribute, and the mean velocity given by Eq. (6c) is expected to give the best fit.

The results of the calculation of $d\sigma^{SEB}/d(\hbar\omega)\,d\Omega_L$ from Eq. (1) for the three values of the mean velocity are shown in Fig. 6 for bombarding energies of 1, 2, 3, and 4 MeV/amu.

Finally, the angular dependence of the bremsstrahlung spectrum from secondary electrons, estimated from Eq. (5), is shown in Fig. 7, where the intensities are normalized at 90°. From this figure it is found that the intensity of the spectrum at about T_m is maximum at 90° and becomes less in the forward and backward directions. This fact reflects the angular distribution of ejected electrons. This energy-dependent directional anisotropy of the bremsstrahlung was also estimated for the two other values of the mean electron velocity of Eqs. (6a) and (6b), showing only a slight change from that of Fig. 7.

It is expected that multiple processes, which have been neglected in this calculation, may flatten out, more or less, the estimated angular dependence; further, we expect that the retardation effect, neglected in Eq. (3), will shift the maximum cross section at 90° to forward directions as the projectile energy gets higher.

B. Bremsstrahlung from projectile

The accelerations which occur during close collisions between the projectile and the nuclei of the target atoms result in a direct production of nuclear bremsstrahlung. The cross section for the production of electric-dipole bremsstrahlung by this process is given by the formula[9]

$$\frac{d\sigma^{br}(\hbar\omega)}{d(\hbar\omega)\,d\Omega_L} = \frac{Z_p^4}{2\pi}\left(\frac{e^2}{m_e c^2}\right)^2 \frac{e^2}{\hbar c}\left(\frac{m_e}{M_p}\right)^2 Z^2 \left(1 - \frac{ZM_p}{Z_p M}\right)^2 \frac{m_p c^2}{(E/\text{amu})} \frac{1}{\hbar\omega} \ln\left[2^{5/2} \frac{\hbar c (E/\text{amu})^{3/2}}{e^2 \hbar\omega (m_p c^2)^{1/2}} \frac{1}{Z}\left(\frac{M_p}{Z_p m_p}\right)\right] (1 + \cos^2\theta_{br}), \quad (7)$$

TABLE I. Comparison of bremsstrahlung-production cross section by nuclear collisions of the projectile $d\sigma^{br}/d(\hbar\omega)\,d\Omega$ with that by secondary electrons $d\sigma^{SEB}/d(\hbar\omega)\,d\Omega$ using $\frac{1}{2}m_e\bar{v}^2 = (Z^2/n^2)\mathcal{R}$.

E/amu (MeV)	$\hbar\omega$ (keV)	$\frac{d\sigma^{br}}{d(\hbar\omega)\,d\Omega}$ (b/keV sr Z^2) p	^{3}He	$\frac{d\sigma^{SEB}}{d(\hbar\omega)\,d\Omega}$ (b/keV sr Z^2)
1	4.0	1.78×10^{-6}	0.243×10^{-6}	2.9×10^{-4}
	3.0	2.50×10^{-6}	0.339×10^{-6}	2.9×10^{-3}
2	5.0	0.81×10^{-6}	0.109×10^{-6}	1.5×10^{-3}

where M is the mass of the target nucleus, Z_p is the charge of the projectile, and m_p is the mass of proton. Higher multipolar radiations are usually of much lower intensity. This cross section for aluminum was evaluated for some values of E/amu and $\hbar\omega$ and is shown in Table I together with the cross section for the bremsstrahlung production by secondary electrons.

Thus, it is found that the bremsstrahlung from the projectile can be neglected compared with that from secondary electrons in the energy region measured here. This fact is consistent with the experimental results shown in Fig. 1, where the measured spectra can be well scaled by $(E/\text{amu})Z_p^2$ as predicted from the BEA and differently from the (Z_p, M_p) dependence shown by Eq. (7).

IV. COMPARISON WITH EXPERIMENTAL RESULTS AND DISCUSSION

In order to compare experimental results with the theoretical calculations, the experimental results were corrected for the x-ray absorption in the target, the Mylar window, the air path, and also for the detection efficiency of the Si(Li) detector as was previously described.[16] The absorption in the Mylar window and the air path was measured experimentally as a function of photon energy.

Comparisons of the experimental results with the theoretical calculations are shown in Fig. 8 for bombarding energies of 1, 2, 3 and 4 MeV/amu, together with the results of calculations by Folkmann *et al.*[1] Here, only the calculations with the mean velocity of Eq. (6c) are shown as this gives the best fit to the experimental results (compare Fig. 6 with Fig. 8). The calculations have also been done for the case of a carbon target and were compared with the experimental results of Folkmann *et al.*,[1] as shown in Fig. 9.

In the calculation of Folkmann *et al.*, the angular distribution of ejected electrons and consequently that of bremsstrahlung, has been neglected, and it has been assumed that $dE/N\,dx \propto 1/E$ and

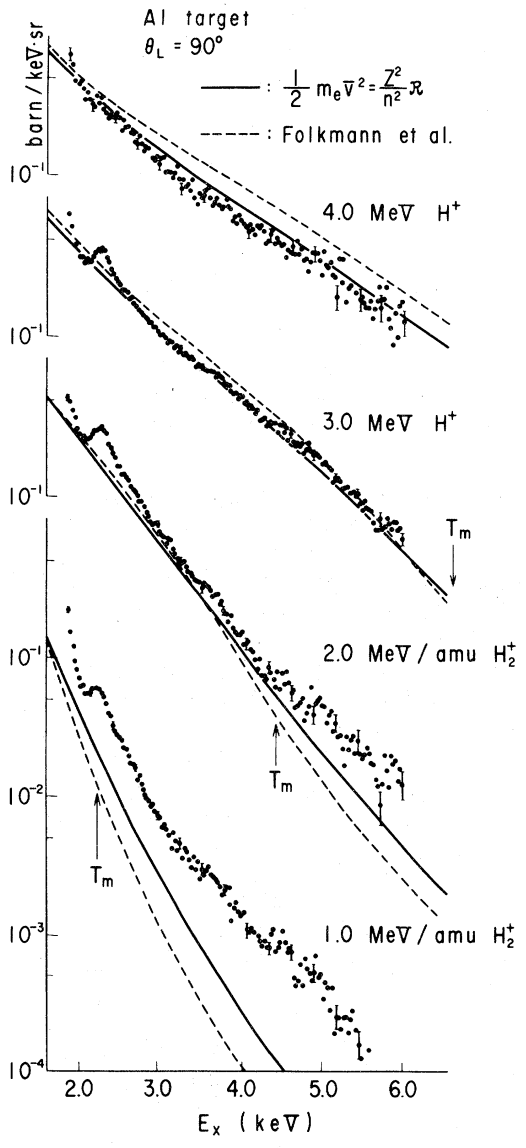

FIG. 8. Comparison of the calculated bremsstrahlung spectra from an aluminum target with the experimental results obtained by 1.0- and 2.0-MeV/amu H_2^+ and 3.0- and 4.0-MeV/amu H^+ bombardments.

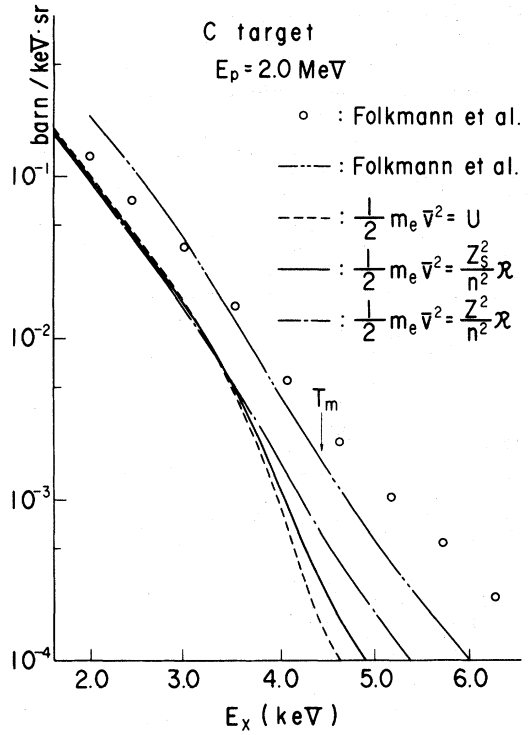

FIG. 9. Comparison of the calculated bremsstrahlung spectra from a carbon target with the experimental results obtained by Folkmann *et al.* (Ref. 1).

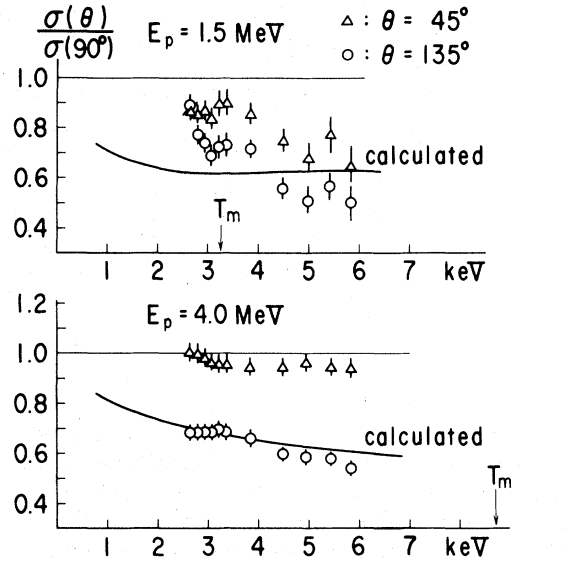

FIG. 10. Ratios of bremsstrahlung-production cross sections measured at 45° and 135° to those at 90° obtained with proton beams of 1.5 and 4.0 MeV.

$d\sigma^{br}/d(\hbar\omega)\,d\Omega \propto 1/E\hbar\omega$, and the calculations contain an uncertainty of a factor of 1.5. Thus, the apparently better agreement with the experimental absolute cross sections for the C target, seen in Fig. 9, might be fortuitous. The present calculation can generally reproduce the experimental results better than that of Folkmann *et al.* over the whole energy range. However, both calculations predict values smaller than the experimental results in the region $T_m < \hbar\omega$. It must be noted that, from Fig. 8, the bremsstrahlung at E/amu = 3 and 4 MeV is produced mainly by electrons ejected from outer shells in the target atom, whereas the bremsstrahlung at lower values of E/amu is produced predominantly by electrons ejected from strongly bound orbitals and the calculations predict smaller production cross sections than the experimental results as the projectile energy gets lower. Therefore, it is suspected that the disagreement between the experimental results and the BEA calculation in the region above T_m might be due to the inadequacy of the BEA for this energy region.

The bremsstrahlung-production cross sections by proton beams of 1.5 and 4.0 MeV have been measured at directions of 45°, 90°, and 135° with respect to the incident beam and the ratios of cross sections obtained at 45° and 135° to those at 90° are shown in Fig. 10 as a function of photon energy together with those calculated from Eq. (5). The experimental anisotropy measured at E_p = 4.0 MeV and 90° and 135° agrees well with the calculated one. However, at the forward direction, the measured cross sections relative to that at 90° are larger than the estimated ones both at E_p = 1.5 and 4.0 MeV. This fact might be due to the retardation effect, which shifts the angle corresponding to the maximum differential cross section to the forward direction at higher incident energy. Thus it is found that the directional anisotropy of the bremsstrahlung is not entirely flattened out by multiple processes in the energy range measured here.

Recently, energy-dependent directional anisotropies of the MO x rays have been observed, assuming an isotropic distribution of background radiations, and are argued as strong evidence for the quasimolecular origin of these radiations.[5,17] It is noted, however, that this identification of the MO x rays from angular dependence of the spectrum should be carefully done, as the MO x rays overlap on the high-energy tail of the bremsstrahlung, which extends to the region of several tens of keV in the cases of heavier elements and is found to show a similar angular dependence.

Moreover, it is clear from the present experiment that the signal-to-noise ratio in a trace-element analysis by characteristic x rays is expected to be improved at backward directions rather than

at the 90° direction, which has usually been adopted.

V. SUMMARY

The bremsstrahlung induced by heavy-charged-particle bombardment of aluminum was calculated based on the binary-encounter model with improved approximations and was compared with the experimental results measured over the bombarding energy range 1–4 MeV/amu. The agreement of the calculation with the experiment was much improved; especially, a good fit to the absolute cross section was obtained without any adjustable parameter. Generally, the theoretical cross section becomes smaller than the experimental cross section as the photon energy becomes higher and the bombarding energy gets lower, i.e., in the region where the secondary electron ejected from inner shells of the target atom plays a predominant role for producing the bremsstrahlung.

The angular dependence of the bremsstrahlung spectrum was estimated and was found theoretically to show the $\sin^2\theta$ dependence at highest photon energy. The calculated results were compared with the experimental results measured with proton beams of 1.5 and 4.0 MeV at the directions of 45°, 90°, and 135°, showing general agreements. It must be noted that the total cross section for the bremsstrahlung production is greatly affected by this angular dependence, and this dependence is to be carefully considered in the identification of MO x rays from their directional anisotropy.

Detailed measurements of angular dependence of the bremsstrahlung-production cross section at other directions and energies are now in progress in our laboratory.

ACKNOWLEDGMENTS

The authors would like to express their sincere gratitude to M. Kato for his skillful operation of the accelerator during the course of this experiment and also to M. Kamiya and K. Sera for their cooperation in taking data.

[1]F. Folkmann, C. Gaarde, T. Huus, and K. Kemp, Nucl. Instrum. Methods 116, 487 (1974).
[2]F. Folkmann, J. Borggreen, and A. Kjeldgaard, Nucl. Instrum. Methods 119, 117 (1974).
[3]W. E. Meyerhof, T. K. Saylor, S. M. Lazarus, W. A. Little, B. B. Triplett, and L. F. Chase, Jr., Phys. Rev. Lett. 30, 1279 (1973).
[4]C. K. Davis and J. S. Greenberg, Phys. Rev. Lett. 32, 1215 (1974).
[5]J. S. Greenberg, C. K. Davis, and P. Vincent, Phys. Rev. Lett. 33, 473 (1974); G. Kraft, P. H. Mokler, and H. J. Stein, Phys. Rev. Lett. 33, 476 (1974); P. Gipper, K. H. Kaun, F. Stary, W. Schulze, and Yu. P. Tretyakov, Nucl. Phys. A 230, 509 (1974); B. Müller and W. Greiner, Phys. Rev. Lett. 33, 496 (1974).
[6]H. Bethe, Z. Phys. 76, 293 (1932).
[7]L. C. L. Yuan and C. S. Wu, *Methods of Experimental Physics* (Academic, New York, 1961), Vol. 5A, p. 10.
[8]Heitler, *The Quantum Theory of Radiation* (Clarendon, Oxford, England, 1954), p. 242.
[9]J. D. Jackson, *Classical Electrodynamics* (Wiley, New York, 1962), p. 505 (Sec. 15); K. Alder, A. Bohr, T. Huus, B. Mottelson, and A. Winther, Rev. Mod. Phys. 28, 432 (1956).
[10]H. K. Tseng and R. H. Pratt, Phys. Rev. A 3, 100 (1971).
[11]J. D. Garcia, Phys. Rev. 177, 223 (1969).
[12]E. Merzbacher and H. W. Lewis, in *Handbuch der Physik*, edited by S. Flügge (Spinger-Verlag, Berlin, 1958), Vol. 34, p. 166.
[13]T. F. M. Bonsen and L. Vriens, Physica (Utr.) 47, 307 (1970).
[14]B. F. J. Schonland, Proc. R. Soc. Lond. A 108, 187 (1925).
[15]M. E. Rudd, C. A. Sautter, and C. L. Bailey, Phys. Rev. 151, 20 (1966).
[16]H. Tawara, K. Ishii, S. Morita, H. Kaji, C. H. Hsu, and T. Shiokawa, Phys. Rev. A 9, 1617 (1974).
[17]R. S. Thoe, I. A. Sellin, M. D. Brown, J. P. Forester, P. M. Griffin, D. J. Pegg, and R. S. Peterson, Phys. Rev. Lett. 34, 64 (1975).